Effective temperature bridges length-scales by facilitating lumped models of heterogeneous battery cells

Mark Blyth[1] and Alastair Hales[2]

[1,2]University of Bristol, UK
[1,2]The Faraday Institution, UK

January 31, 2025

Context and scale

Temperature is immensely important to electrochemists, as it governs the kinetics of electrochemical systems and determines how well a battery system will perform. Temperature measurements are comparatively simple with small coin cells, however challenges start to emerge at larger scales. The combination of self-heating and thermal management means temperature gradients become significant, so that temperature varies throughout cells, modules, and packs. This makes it difficult to define a single temperature measurement, and to compare temperature effects on system performance. To address this, we ask 'what is the most appropriate temperature measure for a heterogeneous battery system?'. The effective, or uniform temperature of a cell has been previously introduced as one such measure. We argue that this is the correct measure for comparing temperature across the length-scales, and develop the necessary frameworks to make use of it. We take care to highlight the full zoo of heterogeneous effects, and to describe the fundamental electrochemistry governing them. These findings will offer great value to battery pack designers, thermal management engineers, and battery management systems. While isothermal models are commonly used in academia and industry, their theoretical justifications are missing in the literature. Our methods provide the necessary theoretical foundations, by providing methods to accurately capture the behaviours of heterogeneous battery systems with lumped models. Our work serves as a bridge between the various length-scales of battery science, from coin cell to pack scale, and presents a suite of conceptual tools for future heterogeneity studies.

Abstract

The kinetics of a battery cell vary with temperature, which causes changes to electrical properties such as power capability and accessible capacity. Knowledge of cell temperature is therefore essential for battery design and operation. However, complications arise since electrochemical systems generate heat, causing thermal gradients to emerge. No single measure of this temperature distribution exists, which hinders battery design and management, and means pack, cell, and coin cell data cannot be directly compared. Here we address this issue, by proposing a temperature measurement of a heterogeneous system that accounts for the effects of the heterogeneity on overall system kinetics. Previous authors have noted that a cell with a temperature gradient shows the same impedance as an identical lumped cell, at some uniform temperature. We refer to this as the effective temperature of a heterogeneous cell. We derive an explicit distributed cell model, consisting of parallel connected Thevenin circuits, from which a formula for effective temperature is defined. This results in a single temperature measurement for a heterogeneous battery system, which gives the temperature value that best represents the overall electrical dynamics, and correctly accounts for uneven temperature distributions. We show how the parameters of a thermal model can be extracted from electrical data, and note that the calibrated model recovers the effective temperature of the cell, despite having not been fitted to temperature data. This shows that our proposed temperature metric is an intrinsic and fundamentally meaningful measurement. Our results enable accurate lumped models of heterogeneous cells and packs, by capturing heterogeneity with effective temperature. In turn, this acts as a bridge to enable direct comparisons of electrochemical systems, regardless of length-scales and heterogeneity.

1 Background

Heat is generated within a cell during operation [1], and thermal management systems are used to ensure temperatures remain within safe ranges. The combination of heat generation and removal causes thermal gradients within cells and batteries. Cell impedance varies with temperature and state of charge [2, 3]. As a result, both temperature and impedance will vary spatially within an operational battery or cell. Due to the coupling between thermal and electrical behaviours, these effects cannot be volume-averaged away [4]. This makes it difficult to directly compare the dynamics of engineering-scale heterogeneous systems against each other, and against small-scale experiments such as coin-cells.

Temperature heterogeneity causes a variety of knock-on effects. Higher temperatures lead to lower cell impedance, meaning higher current densities are typically found in hotter regions. Variations in current density causes variations in the localised state of charge across cells and packs [5, 6]. The resulting state-of-charge gradients can be sustained even when cells are rested, due to hysteretic effects [5]. Heterogeneity can cause performance issues, and is known to accelerate degradation [7, 8, 9]. Challenges also arise for pack design and management. Due to thermal gradients, a temperature measurement on the cell surface will underestimate its operating temperature, resulting in errors in the prediction of terminal voltage and heat generation. These errors propagate through to inaccuracies in state-of-charge and state-of-health estimation, and also lead to the design of overpowered, overly conservative thermal management systems. Pack designers seek maximum lifespan and performance for minimum cost; a detailed understanding of heterogeneity and its impacts is highly valuable for this.

Heterogeneity has received increased attention as companies move towards larger-format cells, which sustain larger thermal gradients. Previous studies cover topics such as tab and cell design [10, 11], thermal management and cooling strategies [12, 13, 14], and cell-to-cell variations within packs [15, 16, 17]. Other researchers have correlated larger heterogeneity with a larger loss of accessible capacity [12]. Nevertheless, it is unclear whether this effect is caused by the heterogeneity itself, or because the system with more heterogeneity was operating at a lower overall temperature, and hence a higher impedance.

Current methods do not allow the effects of temperature and state-of-charge gradients to be decoupled, which motivates a key contribution of our work. We provide a method for calculating the effective temperature of a heterogeneous cell, given a temperature and charge gradient. Effective temperature was previously introduced by Richardson — who refers to it as uniform cell temperature — in a suite of work investigating impedance methods for cell temperature estimation [18, 19, 20, 21]. Effective (or uniform) temperature is defined as the temperature a homogeneous cell must be at, in order to show the same impedance as the heterogeneous cell of interest. Effective temperature provides a meaningful temperature measure for a heterogeneous system, so that systems can be directly compared against each other, and against homogeneous cells, to unpick the impacts of charge and temperature gradients on cell performance.

Distributed models are regularly used for investigating heterogeneous battery systems, whereby full cells are modelled by multiple electrically and thermally connected units, to capture spatial variations inside a cell [22]. While the dynamics of parallel-connected cells have been derived [23], most distributed models are pitched as software-simulators [24, 25, 22] as opposed to explicit closed-form equations. Distributed models have not been used for analytical studies before, which has limited the opportunities to learn about the system dynamics. Our work derives a closed-form distributed model, and demonstrates that rigorous analytical methods are both practical and useful here. Our derivation shows that distributed models are suitable for analytical study, and highlights the benefits of performing mathematical analysis alongside simulations.

We use a closed-form mathematical model of a heterogeneous cell, and study its structure to extract novel insights into the behaviours of heterogeneous systems. The model is used to unpick the causes and effects of heterogeneity, and to motivate effective temperature as a universal temperature metric for heterogeneous battery systems. Our work serves to develop effective temperature as a single, simple measurement to allow direct comparison of electrochemical systems across scales. Furthermore, it builds the necessary frameworks to use effective temperature as a modelling tool, so that a major portion of the dynamics of heterogeneous models can be captured using lumped models. Our discussion highlights the novel insights that our derived equations offer; we summarise these in a diagram, showing the various forms of heterogeneity, their interactions, and the fundamental electrochemistry governing them. Our work thus provides a conceptual framework for understanding heterogeneity at all scales, and provides the necessary tools to reason about it rigorously.

The manuscript is structured as follows. We first introduce our choice of models, then

- a closed-form model of a heterogeneous cell is used to derive an explicit formula for the effective

temperature of a cell;

- we demonstrate that the coupling between thermal and electrical dynamics allows thermal models to be fitted from electrical data;
- we show that the calibrated thermal model recovers the effective cell temperature;
- this is used to explain why effective temperature is a meaningful temperature measure for heterogeneous electrochemical systems.

In Section 2, the equations for a standard lumped model are stated, and used to derive an explicit model of a heterogeneous cell with coupled and spatially varying electrothermal dynamics. The models are then used in Section 3, to compute a formula for the effective temperature of a cell, to propose an experimentally achievable parameterisation procedure for the thermal model, and to demonstrate that such a model fitting procedure yields the cell effective temperature. Section 4 discusses the scope of our results, by highlighting what effects our models can and cannot capture; this leads to a graphical summary of all heterogeneous effects and their underlying physics. Section 5 concludes the work.

2 Cell modelling

We first introduce our choice of homogeneous lumped model, and then generalise it to a heterogeneous cell model capable of capturing coupled, spatially varying temperature and charge profiles. Some readers may choose to jump straight to Section 3, where the models are used for studying heterogeneity.

2.1 Lumped (homogeneous) cell model

We consider a standard n-RC Thevenin equivalent-circuit model [26], as sketched in Fig. 1. Such models are used extensively throughout the literature, and the model structure is amenable to analytical study, which would become intractable with physics-based models. The electrical model has a terminal voltage v_{batt} [V]; nominal capacity Q_{nom} [Ah]; series resistance R_0^{lumped} [Ω]; polarisation resistances R_i^{lumped} [Ω] and capacitances C_i^{lumped} [F]; polarisation overpotentials v_{rc_i} [V] for $i \in \{1, \dots, n_{\text{rc}}\}$; state-of-charge SOC; and open-circuit voltage v_{oc} [V]. Input current $I(t)$ [A] is taken as positive during discharge. The electrical problem is coupled to a lumped thermal model, with thermal mass c [J K^{-1}], heat transfer coefficient h [W K^{-1}], temperature T [°C], and far-field temperature T_∞ [°C]. Dynamics are governed by

$$
\begin{cases}
\dfrac{\mathrm{d}}{\mathrm{d}t}SOC = \dfrac{I(t)}{Q_{\text{nom}}} \ , \\
\quad \dfrac{\mathrm{d}v_{\text{rc}_i}}{\mathrm{d}t} = \dfrac{1}{C_i^{\text{lumped}}(T, SOC)} \left(I(t) - \dfrac{v_{\text{rc}_i}}{R_i^{\text{lumped}}(T, SOC)} \right) \ , \\
\quad \dfrac{\mathrm{d}T}{\mathrm{d}t} = \dfrac{1}{c} \left(\underbrace{I^2(t) R_0^{\text{lumped}}(T, SOC) + \sum_{i=1}^{n_{\text{rc}}} \dfrac{v_{\text{rc}_i}^2}{R_i^{\text{lumped}}(T, SOC)}}_{\text{Irreversible heat generation}} - \underbrace{h(T - T_\infty)}_{\text{Convective heat loss}} \right) \ , \\
v_{\text{batt}}(t) = v_{\text{oc}}(T, SOC) - I(t) R_0^{\text{lumped}}(T, SOC) - \sum_{i=1}^{n_{\text{rc}}} v_{\text{rc}_i} \ .
\end{cases}
\tag{1}
$$

2.2 An explicit model of a heterogeneous cell

While the dynamics of parallel-connected cells is known [23], a full mathematical description of a distributed cell model is missing in the literature. We now address this gap by deriving equations for the full electrothermal dynamics of a cell. Our distributed model generalises the lumped model to include spatial variations. These are modelled using a collection of parallel-connected equivalent circuit branches, as sketched in Fig. 1. Each individual circuit-branch is interpreted as a single layer (or collection of adjacent layers) within a pouch cell[1].

[1] The model and results can also be taken to represent parallel-connected cells in a battery module.

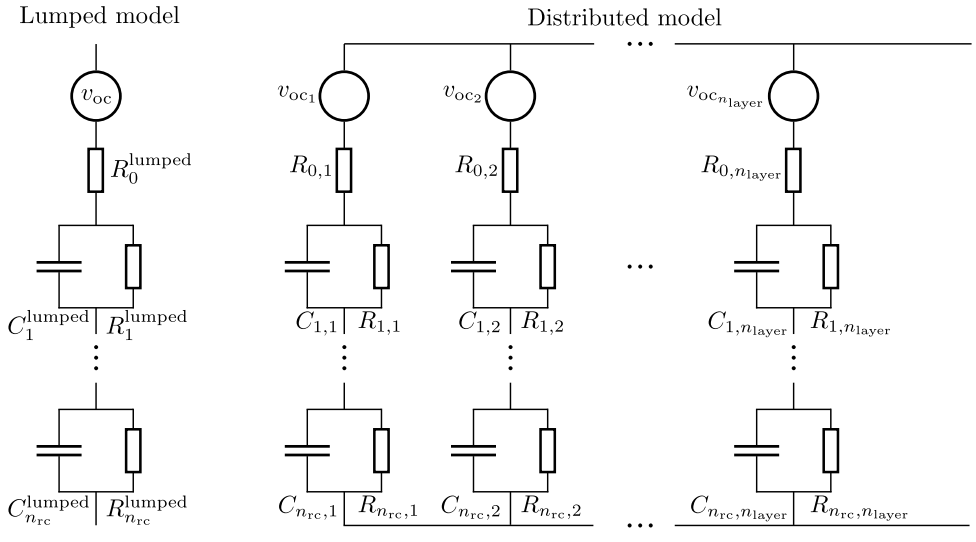

Figure 1: Schematic of the lumped model, and its generalisation to a distributed model. Each parallel strand of the distributed model represents a single layer within a multi-layer cell, and has its own layer-current, state-of-charge, and temperature.

We investigate a cell under one-sided cooling. In such cases, the dominant temperature gradient is across the thickness of the cell, so we choose a one-dimensional model to capture these dynamics. Heat generation in each cell-layer is found from the ohmic losses of an electrical model. These electrical models track state-of-charge, current density, and polarisation overpotentials. Temperature gradients are described using a discretised heat equation. Together, these provide all the necessary information to understand how the heterogeneous cell behaves.

We first introduce the electrical problem. Consider the jth layer of the model, with state-of-charge SOC_j, temperature T_j, and layer-current I_j. Each layer has a capacity of $Q_{\mathrm{nom}}/n_{\mathrm{layer}}$, and hence, layerwise state-of-charge evolves as

$$\frac{\mathrm{d}}{\mathrm{d}t} SOC_j(t) = n_{\mathrm{layer}} \frac{I_j(t)}{Q_{\mathrm{nom}}} \ . \tag{2}$$

The resistances and capacitances of each layer will differ to those of the overall cell. A components-in-parallel argument gives each layer's resistance and capacitance as

$$R_0 = R_0^{\mathrm{lumped}}(T, SOC)\ n_{\mathrm{layer}} \ , \tag{3}$$

$$R_i = R_i^{\mathrm{lumped}}(T, SOC)\ n_{\mathrm{layer}} \ , \tag{4}$$

$$C_i = C_i^{\mathrm{lumped}}(T, SOC)\ /\ n_{\mathrm{layer}} \tag{5}$$

for $i \in \{1, \ldots, n_{\mathrm{rc}}\}$. Such scalings are commonly used in distributed models [27, 12]. Kirchoff's voltage law dictates that the overall cell terminal voltage v_{batt} is related to layer current I_j by

$$v_{\mathrm{batt}}(t) = v_{\mathrm{oc}}\left(SOC_j\left(t\right)\right) + I_j(t) R_0\left(T_j\left(t\right), SOC_j\left(t\right)\right) + \sum_{i=1}^{n_{\mathrm{rc}}} v_{\mathrm{rc}_{i,j}}(t) \tag{6}$$

for each layer j. (For ease of notation, we now drop explicit dependencies t, $T\left(t\right)$, etc..) Rearranging Eq. (6), the current through layer j is

$$I_j = \frac{1}{R_{0,j}} \left(v_{\mathrm{batt}} - v_{\mathrm{oc}_j} - \sum_{i=1}^{n_{\mathrm{rc}}} v_{\mathrm{rc}_{i,j}} \right) \ . \tag{7}$$

By Kirchoff's current law, the current $I(t)$ through the full cell is related to the layer currents I_j by

$$I = \sum_{j=1}^{n_{\mathrm{layer}}} I_j \ . \tag{8}$$

Substituting the layer currents from Eq. (7) into Eq. (8), and rearranging the result for terminal voltage v_{batt}, yields the output equation for a heterogeneous system as

$$v_{\text{batt}}(t) = \frac{\sum_{j=1}^{n_{\text{layer}}} \frac{v_{\text{oc}_j}}{R_{0,j}}}{\sum_{j=1}^{n_{\text{layer}}} \frac{1}{R_{0,j}}} + I(t)\left(\frac{1}{\sum_{j=1}^{n_{\text{layer}}} \frac{1}{R_{0,j}}}\right) + \frac{\sum_{j=1}^{n_{\text{layer}}} \frac{\sum_{i=1}^{n_{\text{rc}}} v_{\text{rc}_{i,j}}}{R_{0_{i,j}}}}{\sum_{j=1}^{n_{\text{layer}}} \frac{1}{R_{0,j}}} \ , \tag{9}$$

where $R_{0,j} := R_0\left(T_j\left(t\right), SOC_j\left(t\right)\right)$ and $v_{\text{oc}_j} := v_{\text{oc}}\left(SOC_j\left(t\right)\right)$ are the series resistance and open-circuit voltage of layer j.

As with the homogeneous model, the overpotential across the ith RC pair of any given layer evolves according to

$$\frac{\mathrm{d}}{\mathrm{d}t} v_{\text{rc}_{i,j}}\left(t\right) = \frac{1}{C_{i,j}}\left(I_j - \frac{v_{\text{rc}_{i,j}}}{R_{i,j}}\right) \ , \tag{10}$$

following the usual notation, whereby $R_{i,j} = R_i\left(T_j\left(t\right), SOC_j\left(t\right)\right)$ and $C_{i,j} = C_i\left(T_j\left(t\right), SOC_j\left(t\right)\right)$ are the resistances and capacitances of the ith RC pair in layer j. Eq. (7) can be substituted into Eq. (10) to give the dynamics of each RC overpotential in terms of known quantities. The overpotential of the ith RC pair of the jth layer is thus given by

$$\frac{\mathrm{d}}{\mathrm{d}t} v_{\text{rc}_{i,j}} = \frac{1}{C_{i,j}}\left(\frac{v_{\text{batt}} - v_{\text{oc}_j} - \sum_{i=1}^{n_{\text{rc}}} v_{i,j}}{R_{0,j}} - \frac{v_{\text{rc}_{i,j}}}{R_{i,j}}\right) \ , \tag{11}$$

with v_{batt} as per Eq. (9). This gives the full system dynamics of the electrical problem as

$$\begin{cases} v_{\text{batt}}(t) = \dfrac{1}{\sum_{j=1}^{n_{\text{layer}}} \frac{1}{R_{0,j}}}\left(\displaystyle\sum_{j=1}^{n_{\text{layer}}} \frac{v_{\text{oc}_j}}{R_{0,j}} + I(t) + \sum_{j=1}^{n_{\text{layer}}} \frac{\sum_{i=1}^{n_{\text{rc}}} v_{\text{rc}_{i,j}}}{R_{0_{i,j}}}\right) \ , & \\ \dfrac{\mathrm{d}}{\mathrm{d}t} SOC_j(t) = n_{\text{layer}} \dfrac{v_{\text{batt}} - v_{\text{oc}_j} - \sum_{i=1}^{n_{\text{rc}}} v_{i,j}}{R_{0,j} Q_{\text{cell}}} \ , & j \in [1, \ldots, n_{\text{layer}}] \\ \dfrac{\mathrm{d}}{\mathrm{d}t} v_{\text{rc}_{i,j}}(t) = \dfrac{1}{C_{i,j}}\left(\dfrac{v_{\text{batt}} - v_{\text{oc}_j} - \sum_{i=1}^{n_{\text{rc}}} v_{i,j}}{R_{0,j}} - \dfrac{v_{\text{rc}_{i,j}}}{R_{i,j}}\right) \ , & i \in [1, \ldots, n_{\text{rc}}] \ . \end{cases} \tag{12}$$

The thermal problem is now introduced. For surface-cooling, the main temperature gradient will occur over the thickness of the cell. We therefore choose a one-dimensional model, to provide a simple description of all the key dynamics. Consider a cell of thickness L [m], with mass m [kg] and constant, isotropic specific heat capacity c_p [J K^{-1} kg^{-1}] and thermal diffusivity $\mathcal{D}$ [m^2 s^{-1}]. For a localised heat generation rate $\dot{Q}(x,t)$ [W], the temperature profile $T(x,t)$ [°C] is governed by

$$\begin{cases} \dfrac{\partial T}{\partial t} = \mathcal{D}\dfrac{\partial^2 T}{\partial x^2} + \dfrac{1}{mc_p}\dot{Q}(x,t) \ , \\ \dfrac{\partial T}{\partial x}\Big|_{x=0} = h_0\big(T(0,t) - T_\infty\big) \ , \\ \dfrac{\partial T}{\partial x}\Big|_{x=L} = -h_L\big(T(L,t) - T_\infty\big) \ , \end{cases} \tag{13}$$

for far-field temperature T_∞ [°C], and coefficients[2] h_0 and h_L [m^{-1}]. Consider the discretisation of $[0, L]$ into nodes $x_1, \ldots, x_{n_{\text{nodes}}}$. We choose to associate each node of the thermal problem with a layer of the electrical problem, and hence, $n_{\text{nodes}} = n_{\text{layer}}$. Applying a method-of-lines discretisation [28] yields

$$\begin{cases} \dfrac{\mathrm{d}T_1}{\mathrm{d}t} = \mathcal{D}\left(\dfrac{T_2 - T_1}{\Delta x^2} + h_0\dfrac{T_1 - T_\infty}{\Delta x}\right) + \dfrac{1}{mc_p}\dot{Q}_1(t) \ , \\ \dfrac{\mathrm{d}T_j}{\mathrm{d}t} = \mathcal{D}\dfrac{T_{j-1} - 2T_j + T_{j+1}}{\Delta x^2} + \dfrac{1}{mc_p}\dot{Q}_j(t) \ , \\ \dfrac{\mathrm{d}T_{n_{\text{layer}}}}{\mathrm{d}t} = \mathcal{D}\left(\dfrac{T_{n_{\text{layer}}-1} - T_{n_{\text{layer}}}}{\Delta x^2} + h_0\dfrac{T_{n_{\text{layer}}} - T_\infty}{\Delta x}\right) + \dfrac{1}{mc_p}\dot{Q}_{n_{\text{layer}}}(t) \ , \end{cases} \tag{14}$$

[2]Coefficient h [m^{-1}] can be obtained from λ/k, for convection coefficient λ [W m^{-2} K^{-1}] and thermal conductivity k [W m^{-1} K^{-1}].

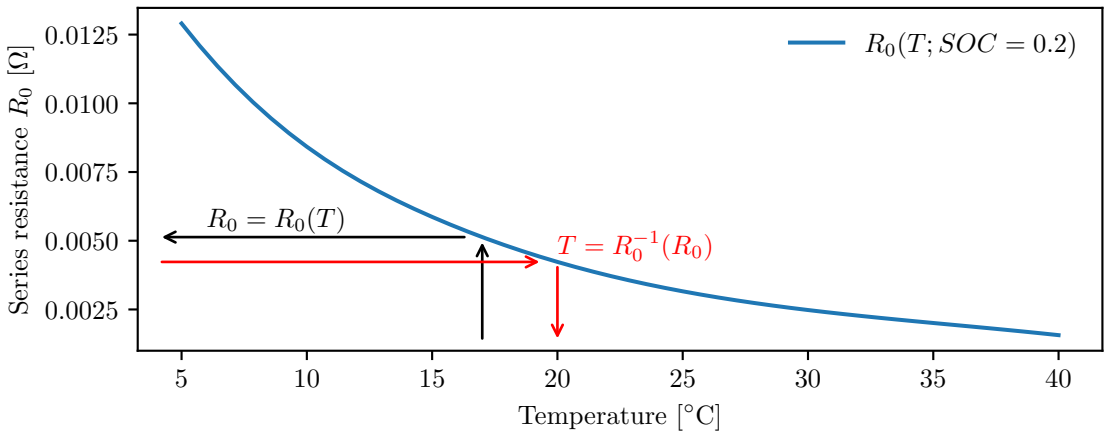

Figure 2: Graphical depiction of the resistance inverse, with experimentally derived series resistance data. $R_0(T; SOC)$ maps a temperature T to a resistance R_0, at some given state-of-charge; its inverse $R_0^{-1}(R_0; SOC)$ maps from resistance back to temperature.

for $T_j = T(x_j, t)$, $\Delta x = 1/(n_{\text{layer}} - 1)$, where $\dot{Q}_j(t)$ is now the heat generated within the finite volume represented by node j. The irreversible heat generation of the jth layer is given by

$$\dot{Q}_j = I_j^2 R_{0,j} + \sum_{i=1}^{n_{\text{rc}}} \frac{v_{\text{rc}_{i,j}}^2}{R_{i,j}} \,. \tag{15}$$

Reversible heating is omitted here as it is not relevant to our following analysis. Nevertheless, it could trivially be included through the addition of an entropy term in Eq. (15) [1].

The heterogeneous cell model is fully defined by the combination of the electrical sub-model, Eqs. (12); the thermal sub-model, Eqs. (14); the heat generation rate, Eq. (15); and a suitable set of initial conditions.

3 Developing effective temperature as a modelling tool

A model for a heterogeneous cell has been derived. We now demonstrate how it can be used to find the effective temperature of a heterogeneous system. To reinforce the value of effective temperature, we then parameterise a lumped thermal model using electrical data; the calibrated model is seen to recover the effective temperature of the cell, showing that it emerges naturally as the correct way to represent the temperature of a heterogeneous system. This also illustrates how the response dynamics of a heterogeneous system can be captured using lumped models. We argue that since effective temperature provides lumped representations of heterogeneous systems, it can be used as a bridge to allow a direct comparison between homogeneous systems such as coin cells, and larger-scale heterogeneous systems such as cells and battery packs.

3.1 Computation of effective temperature

Eq. (12) offers a range of important insights into heterogeneous cell dynamics, which are exploited here to derive an explicit formula for the effective temperature of a cell. The resulting formula produces a single measure to describe heterogeneous cell temperatures, based on the overall impact of temperature and state-of-charge distributions on cell behaviour. The various terms of the output equation in Eq. (12) can be interpreted as

$$v_{\text{batt}}(t) = \underbrace{\frac{\sum_{j=1}^{n_{\text{layer}}} \frac{v_{\text{oc}_j}}{R_{0,j}}}{\sum_{j=1}^{n_{\text{layer}}} \frac{1}{R_{0,j}}}}_{\text{Heterogeneous OCV}} + \underbrace{\left(\frac{1}{\sum_{j=1}^{n_{\text{layer}}} \frac{1}{R_{0,j}}}\right)}_{\text{Emergent series resistance}} I(t) + \underbrace{\frac{\sum_{j=1}^{n_{\text{layer}}} \frac{\sum_{i=1}^{n_{\text{rc}}} v_{\text{rc}_{i,j}}}{R_{0_{i,j}}}}{\sum_{j=1}^{n_{\text{layer}}} \frac{1}{R_{0,j}}}}_{\text{Weighted transient overpotentials}} \,. \tag{16}$$

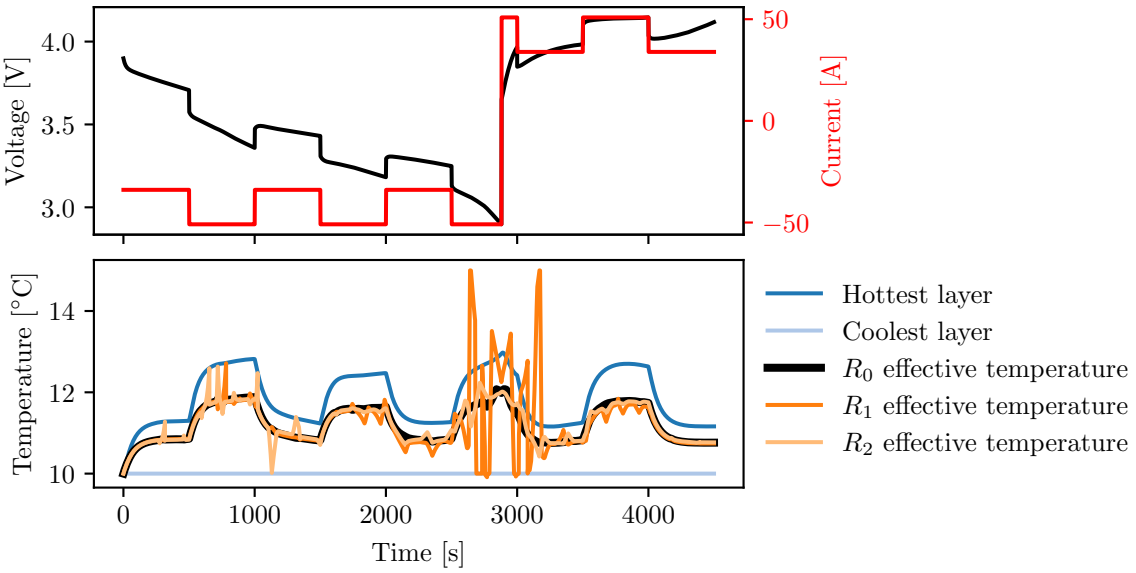

Figure 3: Plot of the drive cycle and associated synthetic data used in this study. Top: a model cell is discharged to 25 % SOC, then charged to upper voltage cutoff. Currents are switched between 0.8 C and 1.2 C every 500 s to induce transients in cell temperature. Bottom: time-series of temperatures at the hottest and coldest layers of the model-cell, and cell effective temperature. Series resistance R_0 leads to the most robust effective temperature calculation, as it is the easiest resistance to parameterise experimentally.

Our derivation focuses on the emergent cell resistance, and how this depends on heterogeneity. Battery cycling experiments and standard model-fitting techniques can be used to extract the overall series resistance $R_0^{\text{lumped}}(T, SOC)$ of a cell. This resistance will decrease monotonically as temperature increases [2, 29, 30]. As a result, a one-to-one mapping emerges between temperature and cell resistance, for a given state-of-charge. By running the mapping in reverse, a cell temperature can be found if the resistance is known. More formally, for temperature T, resistance R_0, and state-of-charge SOC, the inverse mapping is given as

$$T = R_0^{-1}(R_0; SOC) \ , \tag{17}$$

which is sketched in Fig. 2. This can be exploited to find the effective temperature of a cell, provided its emergent series resistance can be found. We note that an equivalent definition could be constructed using polarisation resistances R_i^{lumped}, instead of cell series resistance R_0^{lumped}. As illustrated in Fig. 3, this would yield much the same result. Nevertheless, R_0^{lumped} is easier to parameterise accurately from experiments; errors in the parameterisation of R_i^{lumped} propagate through to errors in the calculated effective temperature, and as such, it is preferable to infer effective temperature from its effects on series resistance. This approach also complements online methods using electrochemical impedance spectroscopy, from which the cell series resistance can be found.

Eq. (16) shows that a heterogeneous cell with temperature profile $T(x_j)$ and state-of-charge profile $SOC(x_j)$ will have an effective series resistance $\tilde{R}_0$ of

$$\tilde{R}_0 = \frac{1}{\sum_{j=1}^{n_{\text{layer}}} \frac{1}{R_0(T_j, SOC_j)}} \ . \tag{18}$$

We can then use the inverse mapping to find the effective cell temperature, by looking for the temperature that gives the emergent resistance $\tilde{R}_0$. Mathematically, effective temperature T_{eff} is found through the combination of Eq. (17) and (18), as

$$T_{\text{eff}} = R_0^{-1}\left(\frac{1}{\sum_{j=1}^{n_{\text{layer}}} \frac{1}{R_0(T_j, SOC_j)}}; SOC\right) \ . \tag{19}$$

This can be immediately generalised to a continuous case for $n_{\text{layer}} \to \infty$.

3.2 Parameterising a thermal model from electrical data recovers cell effective temperature

To validate our findings, we demonstrate that effective temperature naturally emerges as the temperature measure of a heterogeneous cell. First, standard methods are used to fit an equivalent circuit cell model. Once the electrical model is parameterised, it is coupled to a simple thermal model, whose parameters are identified by optimising against voltage predictions. Whilst unusual, this step is shown to be both achievable and practical, since cell resistance and overpotentials depend on the temperature, which is governed by the model's thermal parameters. The full model is seen to produce the effective temperature of a cell. Such behaviour is expected, because maximal voltage-prediction accuracy needs the lumped model to predict the correct emergent resistance for the heterogeneous cell; by definition, effective temperature makes this happen. Results demonstrate the validity of effective temperature, and also provide a practical and useful experimental method.

To create a lumped electrical model, we perform cycling tests on custom-built 2.2 Ah graphite / NMC 622 pouch cells. Peltier elements and PID control are used to maintain the cell surfaces at a constant temperature. Open-circuit voltage curves $v_{\mathrm{oc}}(SOC)$ are found from the relaxations of a pulse discharge test. The electrical sub-model given in Eq. (1) is fitted to each pulse, by using a nonlinear least squares solver to identify parameters R_0, R_1, R_2, C_1, and C_2. Parameterisation is repeated across the state-of-charge range, and at various temperatures. Functional parameters $R_0(T, SOC)$ etc. are then constructed using a bilinear interpolation over the parameters from each pulse. Such methods have reached a high state of maturity [31, 32, 33, 34, 35, 36], and pre-built software tools are available [37]. We scale the resulting model to represent a large format cell, typical of those used in electric vehicles. Following [38], our modelled cell has a geometry of $260 \times 100 \times 11.8$ mm; cell capacity is taken as 42.4 Ah to conserve volumetric capacity density; thermal properties are taken from [39, 40].

The parameterised electrical model is coupled to a lumped thermal model of form

$$\frac{\mathrm{d}T}{\mathrm{d}t} = \frac{1}{c}\Big(\dot{Q}(t) - h(T - T_\infty)\Big) \,. \tag{20}$$

As per Eqs. (1) and (15), $\dot{Q}(t)$ [W] is the heat generation rate predicted by the electrical model; T_∞ [°C] is the cooling system temperature; c [J K^{-1}] is a thermal mass; and h [W K^{-1}] is a heat transfer coefficient. To fit the thermal model, parameters c and h must be found. As introduced previously, we propose a novel fitting method whereby these parameters are identified using electrical data, rather than temperature measurements. This requires a cell or battery system to be cycled in realistic heterogeneous conditions, giving a measured voltage time-series of $v_{\mathrm{hetero}}(t)$. The lumped electrothermal model of Eq. (1) is simulated, yielding predictions $v_{\mathrm{lumped}}(t)$ and prediction error $\|v_{\mathrm{lumped}}(t) - v_{\mathrm{hetero}}(t)\|^2$. A numerical optimiser is used to update the parameter estimates for c and h, thus parameterising the thermal model by solving for

$$\min_{c,h} \|v_{\mathrm{lumped}}(t) - v_{\mathrm{hetero}}(t)\|^2. \tag{21}$$

We use synthetic data for v_{hetero}, as this can be processed to provide a ground-truth effective temperature signal to validate against. Data are generated from simulations a heterogeneous model cell, using Eq. (12) with the electrical parameters previously extracted from pulse discharge tests. Our modelled cell is taken to be insulated on one large face, and held at the cooling-system temperature on the opposite face; such one-sided cooling strategies are regularly used in electric vehicle packs [41, 42, 43]. Synthetic data $v_{\mathrm{hetero}}(t)$ are generated from a current-based drive-cycle, depicted in Fig. 3, which has been designed to aid the identifiability of the thermal parameters. Heat transfer coefficient h controls the relationship between heat input and maximum attained temperature; the product of c and h dictate the timescale over which the cell thermalises. As a result, identification of c relies on transients, so our drive cycle alternates the current magnitude between 0.8 C and 1.2 C every 500 s to induce regular transient changes in the cell temperature.

As shown in Fig. 4, the thermal model reproduces the effective temperature calculated with Eq. (19). Effective temperature thus emerges naturally from the thermal model calibration, which is a notable result since the thermal model is fitted only from current-voltage data. As such, it validates our claim that effective temperature is the most natural and meaningful temperature measure to use, when describing heterogeneous cells. A useful consequence is that effective temperature and cell thermal properties can be reliably recovered from electrical data, without the need for costly, difficult, and time-consuming thermal testing.

To illustrate the commercial relevance of our results, and to further-validate our methods, we now study the performance of our electrothermal model on an electric vehicle drive-cycle. As before, het-

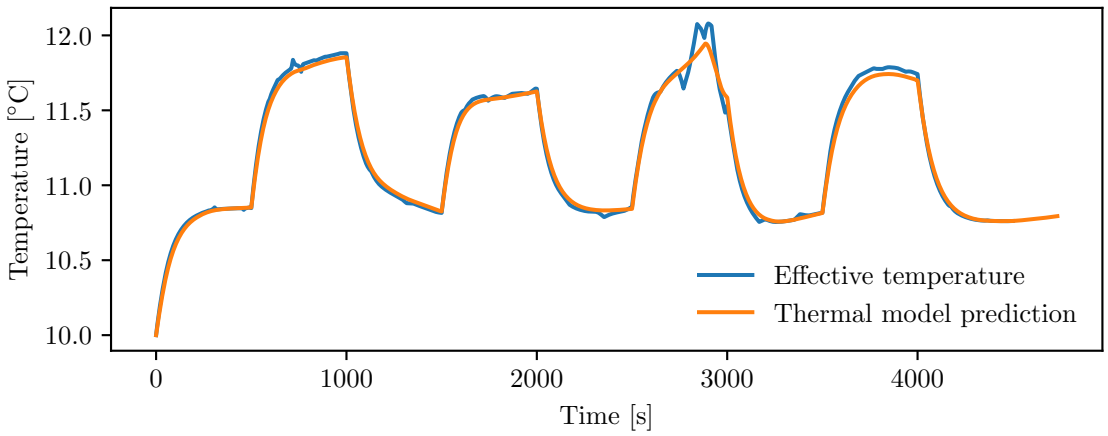

Figure 4: Comparison of calculated effective temperature of a heterogeneous cell, and temperature predictions of a lumped model parameterised entirely from electrical data. The lumped model recovers the effective temperature. This confirms that effective temperature is the correct measure of heterogeneous cell temperature, and demonstrates how it can be recovered from standard cell-cycling tests.

erogeneous data are generated using Eq. (12) to allow a full validation against a known effective temperature. Fig. 5 shows predictions of the calibrated model lumped model, which are compared against heterogeneous simulations from a distributed model. We also compare against a lumped model at constant temperature, which is included as a baseline to represent standard methods where models are supplied with the temperature set-point of the thermal management system. The prediction errors in cell overpotential are computed[3], taking the distributed model results as ground-truth. Our calibrated electrothermal model is significantly more accurate than an isothermal lumped model, indicating that heterogeneous cell dynamics can be modelled accurately with simple and computationally fast lumped models when our effective temperature methods are used. As before, Fig. 6 shows that the lumped thermal model reproduces the effective temperature of the distributed model, despite having not been fitted to any thermal data.

4 Discussion

We have demonstrated how to calculate the effective temperature of a cell, confirmed its validity as a measurement, and shown that it is a feasible modelling tool for experimental systems. We now discuss the broader scope of our work, by discussing the benefits of our methods, exploring the challenges and opportunities in deploying our findings experimentally, and elucidating the full range of macroscale heterogeneous effects that an electrochemical system can display.

4.1 Benefits of modelling with effective temperature

High-performance battery management requires high performance models. The wide temperature range within an operational cell is highlighted in Fig. 6. Core temperature reflects the combination of heat generation and heat rejection abilities. While knowledge of hot-spot temperatures is useful for ensuring safe pack operation, their usage in electrical modelling would lead to underestimating cell resistance, and overestimating performance. Conversely, surface temperature is governed primarily by the thermal management system, and would lead to overestimation of cell resistance and underestimation of performance. Effective temperature lies between these two extremes, and provides the correct temperature measurement for accurate management and control of heterogeneous cells.

Correct temperature characterisation leads to better lumped models. As shown in Fig. 5, a lumped model using effective temperature provides near-identical predictions to a distributed model. Notably, the lumped model has the advantage of being computationally cheap enough to run in real-time on battery management systems. In contrast, distributed models come with higher computational needs,

[3]Overpotentials are calculated relative to the 'true' open-circuit voltage $v_{oc}(SOC)$, not the heterogeneous generalisation proposed in Eq. (16).

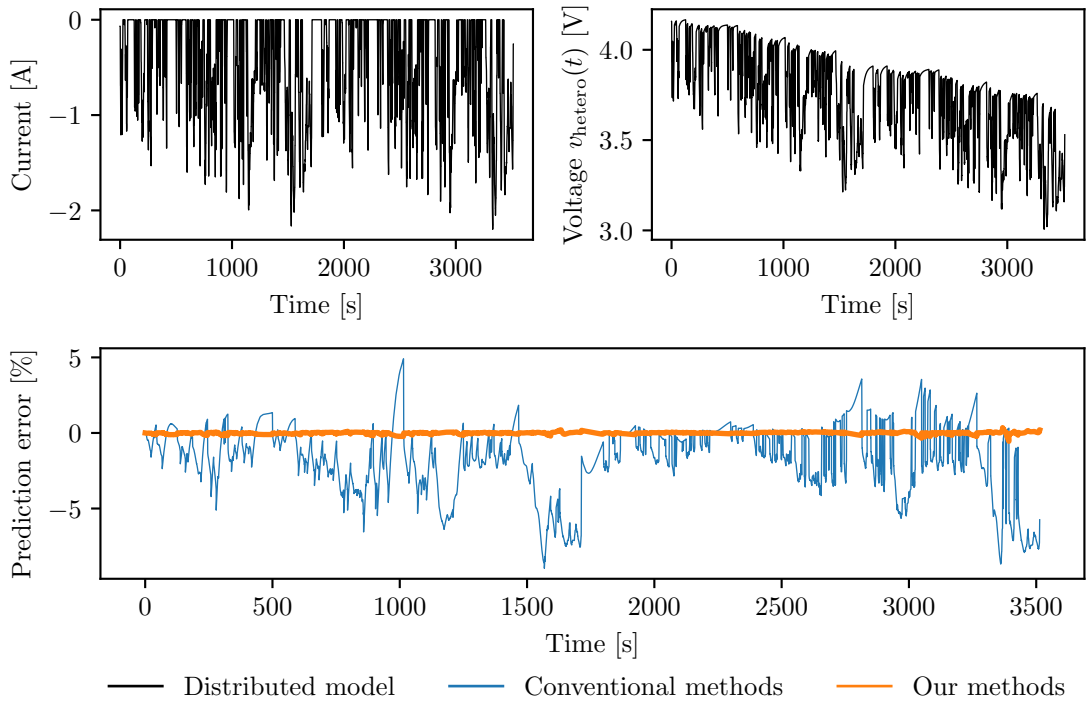

Figure 5: Distributed model simulations of a heterogeneous cell (black) are taken as a reference dataset, and used to calculate the overpotential prediction errors for a lumped isothermal model representing standard modelling methods (blue), and the calibrated lumped electrothermal model introduced in this work (orange). Our model performs substantially better than standard methods for modelling heterogeneous systems, because its thermal model predicts effective temperature.

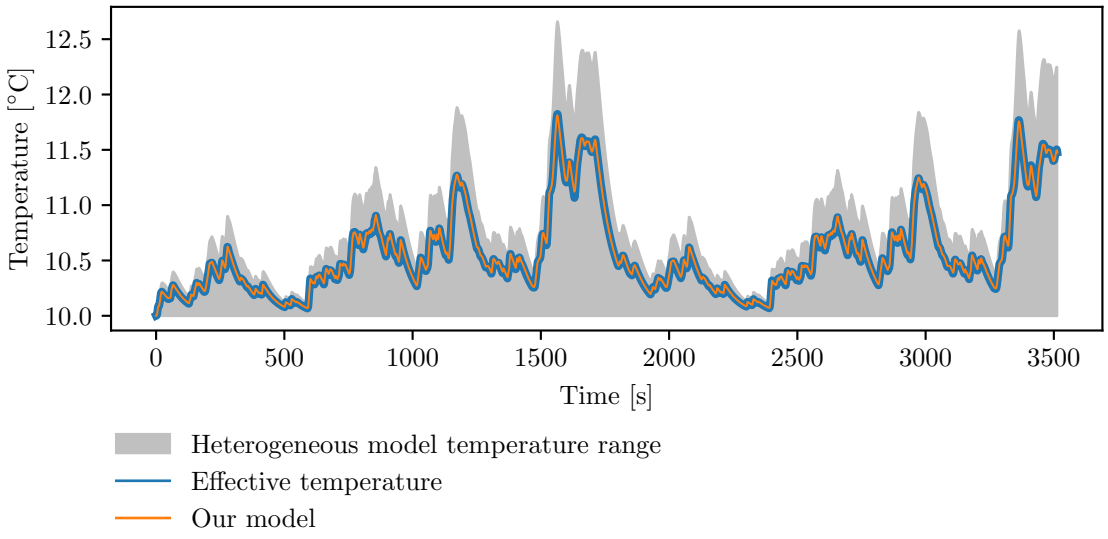

Figure 6: Comparison of temperature predictions for a distributed model, and our calibrated lumped model. Distributed models capture heterogeneity, and exhibit a temperature distribution (grey). Effective temperature can be used as a single temperature measure for this distribution (blue). Our thermal model reproduces cell effective temperature (orange), despite only being fitted to electrical data, reinforcing the validity of both effective temperature and our model parameterisation method.

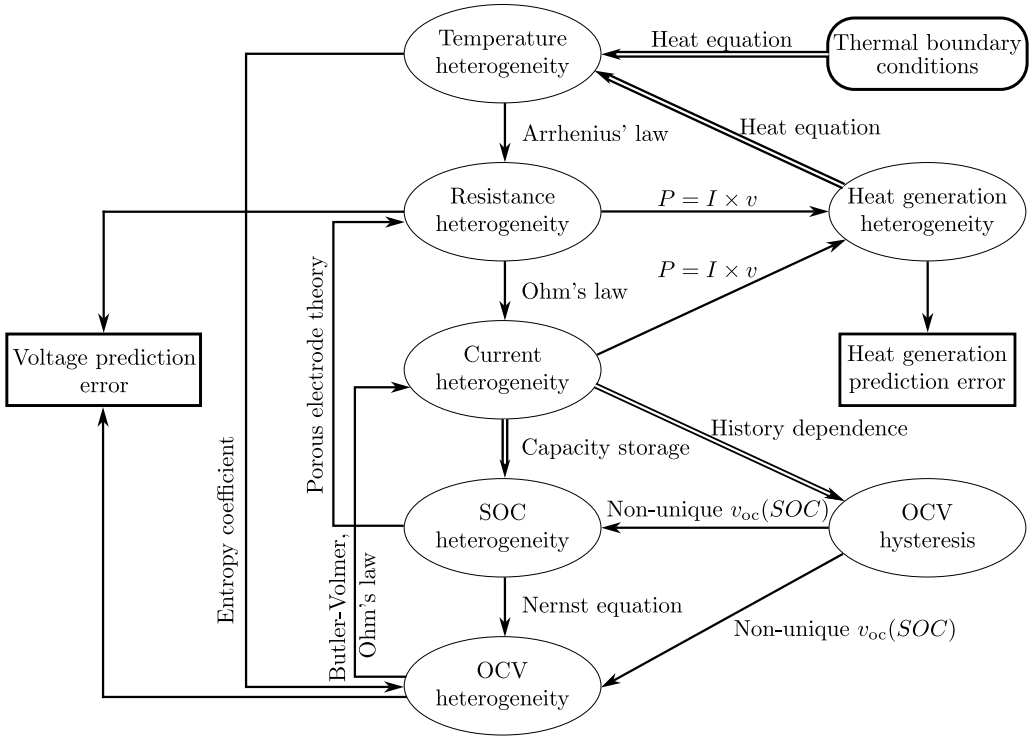

Figure 7: 'Network of heterogeneity', showing how the various internal states of a cell interact, the fundamental electrochemistry governing those interactions, and their results on overall cell performance. First-order effects are shown with a single arrow, eg. a change in resistance leads to an instantaneous change in current; second-order effects are shown with double-arrows; eg. a change in heat generation results in a change to future temperature profiles.

limiting their usage to cell and pack design. Effective temperature modelling retains the accuracy of distributed models and the computational speed of lumped models. The resulting accuracy will unlock opportunities for higher performance pack balancing and management algorithms, leading to improved pack life span and performance.

4.2 Modelling and parameter uncertainties

The work presented here studies synthetic data, generated from a known model. When moving to experimental applications, there will inevitably be small modelling errors between the lumped model and homogeneous experimental dynamics. These additional sources of modelling error may make it more challenging to identify the effective temperature of a heterogeneous cell. Closed-loop state observers are useful to reduce the impacts of such modelling errors, by combining models with data in a statistically optimal manner. The thermal model and parameters identified with our methods are known to be compatible with Kalman-style filters, which can be used to achieve this [19].

An additional source of error arises as the specific heat capacity of real cells is known to change with temperature, amongst other factors [44]. This dependency could easily be captured in Eq. (20) by expanding the thermal mass c as $c = \alpha + \beta T$; then, parameters α and β would be identified instead of c itself, using the same methods as presented here. This framework can optionally be extended further, by including a state-of-charge dependency.

4.3 Further sources of heterogeneity

Heterogeneity is driven by spatial variations in temperature, which cause a range of knock-on effects. We categorise each of these, including their causes, effects, and governing physical principles, in Fig. 7. The combination of heat generation and thermal boundary conditions gives rise to temperature gradients. Temperature causes changes to the cell resistance, governed primarily by Arrhenius' law [2]. In turn, changes to resistance lead to immediate changes in the localised current density, and heat generation rate. Direct couplings such as these are denoted by a single arrow in Fig. 7. The resulting variation

in current density causes different parts of the cell to charge and discharge at different rates, so that variations in the localised state-of-charge emerge. Charge gradients accumulate gradually during cell operation; Fig. 7 indicates these second-order effects using double arrows. Hysteretic effects allow the state-of-charge gradient to persist even in rested cells [5]. Local cell resistivity depends on the local state-of-charge, due largely to the fact that charge-transfer resistance depends on the relative lithiations of each electrode; porous electrode theory describes these dynamics [45, 46, 47]. Charge gradients thus form a feedback loop, whereby changes to state-of-charge drive changes to resistance, changes to resistance cause changes to current density, and changes to current density modify the charge gradients. Open-circuit voltage is subject to similar couplings, whereby it depends on both temperature and local state-of-charge. Open-circuit voltage partially governs electrode overpotentials, and current density depends on the electrode overpotential, as modelled with Butler-Volmer kinetics. Variations in the local open-circuit voltage therefore lead to an additional source of variations in the local current density, driving a further feedback loop. Lumped models that ignore these dynamics will lose prediction accuracy.

Empirical distributed models capture the coupling between heterogeneous effects using various constitutive relationships. Consider again Eq. (16). The emergent series resistance captures the cumulative effects of temperature and state-of-charge heterogeneity, and their effects on localised resistance, and hence, current density. Similarly, the transient overpotentials term approximates the impacts of heterogeneity on polarisation processes and diffusion rates within a cell. A heterogeneous open-circuit voltage emerges, which depends on the magnitude, shape, and direction of the temperature and state-of-charge gradients.

Effective temperature captures key effects of heterogeneity in lumped models, by defining a temperature measure that links heterogeneity to cell performance. However, some effects cannot be captured with this framework. Heterogeneity of resistance and current-density mean that during prolonged charge, state-of-charge gradients will generally 'align' with temperature gradients — hotter areas will have higher charge, and colder areas will have lower charge. Conversely, the charge gradient will typically lie in the opposite direction during discharge — hotter areas will have lower charge, and colder areas will have higher charge. As captured in Eq. (16), cell dynamics will be different between these two cases, however our lumped effective temperature model does not capture state-of-charge gradients. Nevertheless, numerical work suggests these gradients only have a small impact on model prediction accuracy, even at high C-rates. As such, our modelling framework captures the key driver of heterogeneous dynamics — thermal effects — and therefore retains very high accuracy.

5 Conclusion

Lumped models are regularly used in battery science, which assume uniformity in properties such as cell temperature and state-of-charge. However, real cells operate with temperature gradients, due to self-heating effects. Electrochemical kinetics vary with temperature, which results in different electrochemical dynamics at different places in a cell. This makes it difficult to compare results across length-scales, as these spatial variations mean a heterogeneous battery pack will behave differently to a homogeneous coin cell, for example. We introduce effective temperature as a tool to account for these effects. It serves as a simple, single temperature measurement which represents the impacts of thermal and state-of-charge gradients on an electrochemical system. The effective temperature of a cell is the temperature which a hypothetical spatially uniform cell would need to be at, to exhibit the same impedance as a heterogeneous cell at the same overall state-of-charge. We provide a formula to calculate effective temperature, which provides a conceptual bridge from lab-scale electrochemical experiments all the way up to engineering-scale battery packs. Additionally, we develop effective temperature as a modelling tool, and show how it allows the dynamics of heterogeneous cells to be captured using lumped models. Methods are also developed to facilitate its deployment in experiments.

The effective temperature of a heterogeneous cell is chosen such that the associated electrical problem becomes as accurate as possible. We show how this enables thermal models to be parameterised from only electrical data. Such data can easily be obtained from a battery cycler, and expensive testing of thermal diffusivity and heat capacity are not required using our methods. Validation work demonstrates that our calibrated thermal model recovers the effective temperature of a distributed model, and demonstrates that effective temperature really does result in the highest accuracy for the electrical problem. Furthermore, we argue that effective temperature is a fundamental measure of the cell behaviour, since it emerges naturally from the electrical responses of a cell. Lumped models using effective temperature are shown to provide comparable accuracy to distributed models. This demonstrates that effective temperature allows a heterogeneous system such as a pack to be described by, compared against, and equated to

homogeneous systems such as a coin cell. We conclude that, since effective temperature captures the effects of heterogeneity in a single measurement, is the right tool for comparing electrochemical dynamics across all scales of system.

Data and code availability

(All data and code required to reproduce this manuscript will be made publicly available upon publication.)

Author contributions

Methodology, investigation, software, formal analysis, writing — original draft, visualisation: MB. Conceptualisation, resources: MB, AH. Supervision, writing — review and editing, funding acquisition: AH.

Declaration of interests

The authors declare that they have no conflicts of interest.

Acknowledgements

MB and AH are funded by the Faraday Institution Multi Scale Modelling project (grant number: FIRG059), and two EPSRC IAA projects (grant number: A100419).

References

[1] D. Bernardi, E. Pawlikowski, and J. Newman, "A general energy balance for battery systems," *Journal of the electrochemical society*, vol. 132, no. 1, p. 5, 1985.

[2] M. Alipour, C. Ziebert, F. V. Conte, and R. Kizilel, "A review on temperature-dependent electrochemical properties, aging, and performance of lithium-ion cells," *Batteries*, vol. 6, no. 3, p. 35, 2020.

[3] M. Schönleber, C. Uhlmann, P. Braun, A. Weber, and E. Ivers-Tiffée, "A consistent derivation of the impedance of a lithium-ion battery electrode and its dependency on the state-of-charge," *Electrochimica Acta*, vol. 243, pp. 250–259, 2017.

[4] Y. Troxler, B. Wu, M. Marinescu, V. Yufit, Y. Patel, A. J. Marquis, N. P. Brandon, and G. J. Offer, "The effect of thermal gradients on the performance of lithium-ion batteries," *Journal of Power Sources*, vol. 247, pp. 1018–1025, 2014.

[5] M. Fleckenstein, O. Bohlen, M. A. Roscher, and B. Bäker, "Current density and state of charge inhomogeneities in li-ion battery cells with lifepo4 as cathode material due to temperature gradients," *Journal of Power Sources*, vol. 196, no. 10, pp. 4769–4778, 2011.

[6] M. P. Klein and J. W. Park, "Current distribution measurements in parallel-connected lithium-ion cylindrical cells under non-uniform temperature conditions," *Journal of The Electrochemical Society*, vol. 164, no. 9, p. A1893, 2017.

[7] S. Paarmann, K. Schuld, and T. Wetzel, "Inhomogeneous aging in lithium-ion batteries caused by temperature effects," *Energy Technology*, vol. 10, no. 11, p. 2200384, 2022.

[8] S. Li, C. Zhang, Y. Zhao, G. J. Offer, and M. Marinescu, "Effect of thermal gradients on inhomogeneous degradation in lithium-ion batteries," *Communications Engineering*, vol. 2, no. 1, p. 74, 2023.

[9] M. Naylor Marlow, J. Chen, and B. Wu, "Degradation in parallel-connected lithium-ion battery packs under thermal gradients," *Communications Engineering*, vol. 3, no. 1, p. 2, 2024.

[10] T. G. Tranter, R. Timms, P. R. Shearing, and D. Brett, "Communication—prediction of thermal issues for larger format 4680 cylindrical cells and their mitigation with enhanced current collection," *Journal of The Electrochemical Society*, vol. 167, no. 16, p. 160544, 2020.

[11] Y. Zhao, L. B. Diaz, Y. Patel, T. Zhang, and G. J. Offer, "How to cool lithium ion batteries: optimising cell design using a thermally coupled model," *Journal of The Electrochemical Society*, vol. 166, no. 13, pp. A2849–A2859, 2019.

[12] Y. Zhao, Y. Patel, T. Zhang, and G. J. Offer, "Modeling the effects of thermal gradients induced by tab and surface cooling on lithium ion cell performance," *Journal of The Electrochemical Society*, vol. 165, no. 13, pp. A3169–A3178, 2018.

[13] S. Li, N. Kirkaldy, C. Zhang, K. Gopalakrishnan, T. Amietszajew, L. B. Diaz, J. V. Barreras, M. Shams, X. Hua, Y. Patel, *et al.*, "Optimal cell tab design and cooling strategy for cylindrical lithium-ion batteries," *Journal of Power Sources*, vol. 492, p. 229594, 2021.

[14] X. Gao, Y. Li, H. Wang, X. Liu, Y. Wu, S. Yang, Z. Zhao, and M. Ouyang, "Probing inhomogeneity of electrical-thermal distribution on electrode during fast charging for lithium-ion batteries," *Applied Energy*, vol. 336, p. 120868, 2023.

[15] X. Liu, W. Ai, M. N. Marlow, Y. Patel, and B. Wu, "The effect of cell-to-cell variations and thermal gradients on the performance and degradation of lithium-ion battery packs," *Applied Energy*, vol. 248, pp. 489–499, 2019.

[16] C. Pastor-Fernandez, T. Bruen, W. D. Widanage, M.-A. Gama-Valdez, and J. Marco, "A study of cell-to-cell interactions and degradation in parallel strings: implications for the battery management system," *Journal of Power Sources*, vol. 329, pp. 574–585, 2016.

[17] K. Bhaskar, A. Kumar, J. Bunce, J. Pressman, N. Burkell, N. Miller, and C. D. Rahn, "Heterogeneity-induced power and capacity loss in parallel-connected cells," *IEEE Transactions on Transportation Electrification*, 2024.

[18] R. R. Richardson, P. T. Ireland, and D. A. Howey, "Battery internal temperature estimation by combined impedance and surface temperature measurement," *Journal of Power Sources*, vol. 265, pp. 254–261, 2014.

[19] R. R. Richardson and D. A. Howey, "Sensorless battery internal temperature estimation using a kalman filter with impedance measurement," *IEEE Transactions on Sustainable Energy*, vol. 6, no. 4, pp. 1190–1199, 2015.

[20] R. R. Richardson, S. Zhao, and D. A. Howey, "On-board monitoring of 2-d spatially-resolved temperatures in cylindrical lithium-ion batteries: Part ii. state estimation via impedance-based temperature sensing," *Journal of Power Sources*, vol. 327, pp. 726–735, 2016.

[21] R. Richardson, *Impedance-based battery temperature monitoring.* PhD thesis, University of Oxford, 2016.

[22] S. Li, S. K. Rawat, T. Zhu, G. J. Offer, and M. Marinescu, "Python-based equivalent circuit network (pyecn) modelling framework for lithium-ion batteries: next generation open-source battery modelling framework for lithium-ion batteries," 2023.

[23] T. Bruen and J. Marco, "Modelling and experimental evaluation of parallel connected lithium ion cells for an electric vehicle battery system," *Journal of Power Sources*, vol. 310, pp. 91–101, 2016.

[24] C. Veth, D. Dragicevic, R. Pfister, S. Arakkan, and C. Merten, "3d electro-thermal model approach for the prediction of internal state values in large-format lithium ion cells and its validation," *Journal of The Electrochemical Society*, vol. 161, no. 14, p. A1943, 2014.

[25] J. B. Gerschler, F. N. Kirchhoff, H. Witzenhausen, F. E. Hust, and D. U. Sauer, "Spatially resolved model for lithium-ion batteries for identifying and analyzing influences of inhomogeneous stress inside the cells," in *2009 IEEE Vehicle Power and Propulsion Conference*, pp. 295–303, IEEE, 2009.

[26] G. L. Plett, *Battery management systems, Volume I: Battery modeling.* Artech House, 2015.

[27] R. Arunachala, C. Parthasarathy, A. Jossen, and J. Garche, "Inhomogeneities in large format lithium ion cells: A study by battery modelling approach," *ECS Transactions*, vol. 73, no. 1, p. 201, 2016.

[28] S. Hamdi, W. E. Schiesser, and G. W. Griffiths, "Method of lines," *Scholarpedia*, vol. 2, no. 7, p. 2859, 2007.

[29] D. Andre, M. Meiler, K. Steiner, C. Wimmer, T. Soczka-Guth, and D. Sauer, "Characterization of high-power lithium-ion batteries by electrochemical impedance spectroscopy. i. experimental investigation," *Journal of Power Sources*, vol. 196, no. 12, pp. 5334–5341, 2011.

[30] S. Hossain Ahmed, X. Kang, and S. Bade Shrestha, "Effects of temperature on internal resistances of lithium-ion batteries," *Journal of energy resources technology*, vol. 137, no. 3, p. 031901, 2015.

[31] N. Tian, Y. Wang, J. Chen, and H. Fang, "One-shot parameter identification of the thevenin's model for batteries: Methods and validation," *Journal of Energy Storage*, vol. 29, p. 101282, 2020.

[32] M. Lagraoui, M. Lhayani, A. Nejmi, and A. Abbou, "A new method for identifying the parameters of the li-ion battery thevenin model," in *2024 4th International Conference on Innovative Research in Applied Science, Engineering and Technology (IRASET)*, pp. 1–5, IEEE, 2024.

[33] M. Hossain, S. Saha, M. E. Haque, M. T. Arif, and A. M. T. Oo, "A parameter extraction method for the thevenin equivalent circuit model of li-ion batteries," in *2019 IEEE Industry Applications Society Annual Meeting*, pp. 1–7, IEEE, 2019.

[34] S. Jiang, "A parameter identification method for a battery equivalent circuit model," tech. rep., SAE Technical Paper, 2011.

[35] R. Jackey, M. Saginaw, P. Sanghvi, J. Gazzarri, T. Huria, and M. Ceraolo, "Battery model parameter estimation using a layered technique: an example using a lithium iron phosphate cell," tech. rep., SAE Technical Paper, 2013.

[36] J. Knox, M. Blyth, and A. Hales, "Advancing state estimation for lithium-ion batteries with hysteresis through systematic extended kalman filter tuning," *Scientific Reports*, vol. 14, no. 1, p. 12472, 2024.

[37] T. Zhu, R. Tomlin, C. Garcia, S. Rawat, T. Holland, G. Offer, and M. Marinescu, "Lithium-ion battery model parametrisation: Batpar an all-in-one toolkit for equivalent circuit models," *Journal of Energy Storage*, vol. 92, p. 112220, 2024.

[38] Y. Xie, A. Hales, R. Li, X. Feng, Y. Patel, and G. Offer, "Thermal management optimization for large-format lithium-ion battery using cell cooling coefficient," *Journal of The Electrochemical Society*, vol. 169, no. 11, p. 110511, 2022.

[39] K. O'Regan, F. B. Planella, W. D. Widanage, and E. Kendrick, "Thermal-electrochemical parameters of a high energy lithium-ion cylindrical battery," *Electrochimica Acta*, vol. 425, p. 140700, 2022.

[40] G. White, A. Hales, Y. Patel, and G. Offer, "Novel methods for measuring the thermal diffusivity and the thermal conductivity of a lithium-ion battery," *Applied Thermal Engineering*, vol. 212, p. 118573, 2022.

[41] W. Koetting, K. Tom, M. Klein, P. Patil, and K. Kebl, "Battery cell assembly and method for assembling the battery cell assembly," 2014. US Patent US20090186265A1.

[42] J. Blumka, P. Laurain, and A. Jeffrey Smith, "Battery pack," 2018. US Patent US9966641B2.

[43] S. Ketkar, P. Laurain, and R. McCormick, "Battery system and method for cooling the battery system," June 28 2016. US Patent US9379420B2.

[44] L. Tendera, G. K. Mertin, C. Gonzalez, D. Wycisk, A. Fill, and K. P. Birke, "Comprehensive analysis of parametric effects on the specific heat capacity of pristine and aged lithium-ion cells," *Energy Storage and Applications*, vol. 1, no. 1, pp. 35–53, 2024.

[45] J. Newman and W. Tiedemann, "Porous-electrode theory with battery applications," *AIChE Journal*, vol. 21, no. 1, pp. 25–41, 1975.

[46] J. P. Meyers, M. Doyle, R. M. Darling, and J. Newman, "The impedance response of a porous electrode composed of intercalation particles," *Journal of The Electrochemical Society*, vol. 147, no. 8, p. 2930, 2000.

[47] S. Devan, V. R. Subramanian, and R. E. White, "Analytical solution for the impedance of a porous electrode," *Journal of The Electrochemical Society*, vol. 151, no. 6, p. A905, 2004.